Supplementary Data

Ultrafine Fiber-Mediated Transvascular Interventional Photothermal Therapy Using Indocyanine Green for Precision Embolization Treatment

Yingao Ma, †[a] Jingyu Xiao, †[a] Gina Jinna Chen,[b] Hong Dang,[b] Yaran Zhang,[a] Xiaoqin He,[a] Perry Ping Shum,[b] and Qiongyu Guo*[a]

[a]Shenzhen Key Laboratory of Smart Healthcare Engineering, Guangdong Provincial Key Laboratory of Advanced Biomaterials, Department of Biomedical Engineering, Southern University of Science and Technology, 1088 Xueyuan Boulevard, Shenzhen, Guangdong 518055, China.

[b] State Key Laboratory of Optical Fiber and Cable Manufacture Technology, Guangdong Key Laboratory of Integrated Optoelectronics Intellisense, Department of EEE, Southern University of Science and Technology, Shenzhen 518055, China.

†These authors equally contributed to this study.

*Corresponding author: guoqy@sustech.edu.cn (Q. Guo)

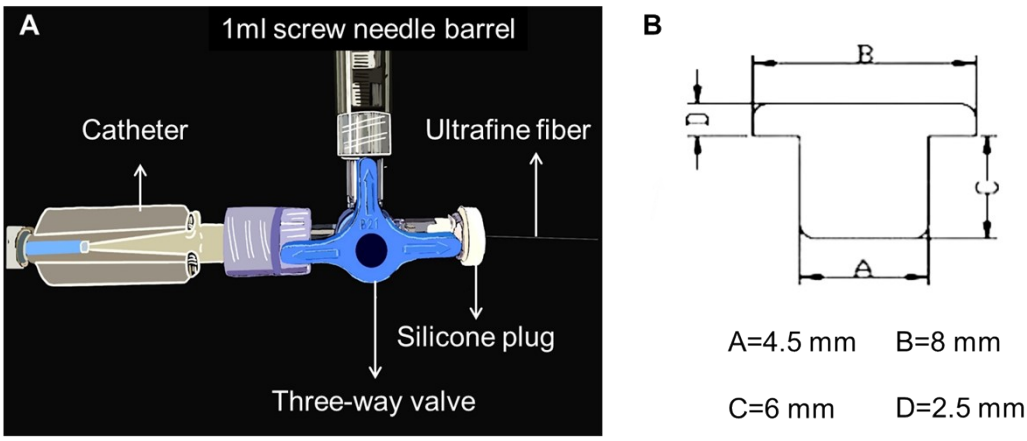

Figure S1. Diagram of assembling a photothermal microcatheter. (A) The three-way valve was connected to the ultrafine fiber through a silicone plug. (B) Size diagram of T-type silicone plug.

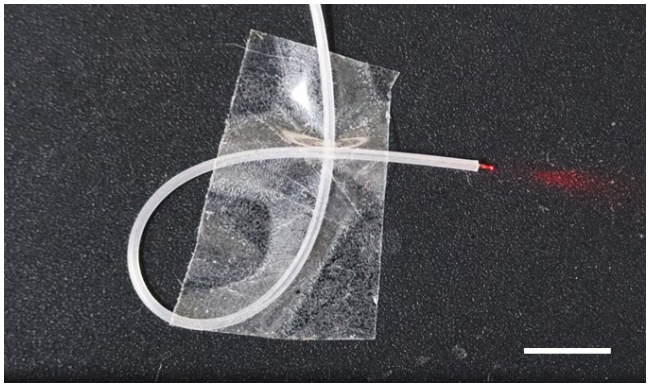

Figure S2. The microcatheter maintains good bendability and compliance. A photograph of the catheter tip showing good bendability (radius of curvature < 10 mm). Scale bar: 5 mm.

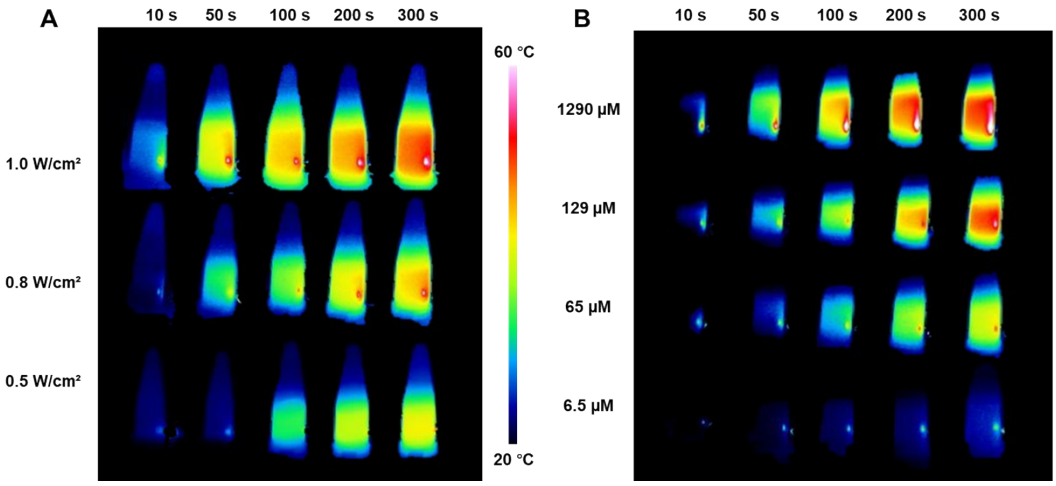

Figure S3. Photothermal characterizations of ICG solution. (A) Infrared imaging of ICG solution with the passage of time under different power densities. (B) Infrared imaging of ICG solution with the passage of time under different ICG solution concentrations.

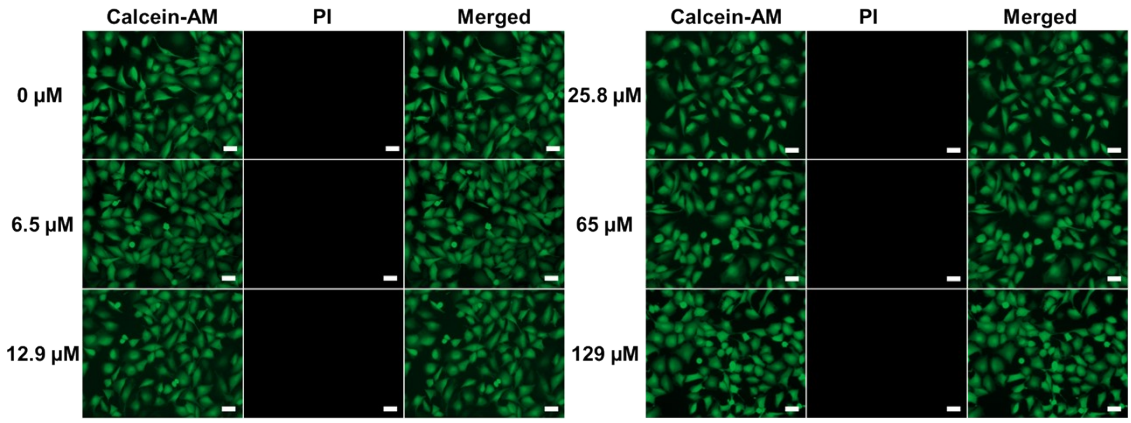

Figure S4. Cytotoxicity of ICG solution. Live/dead cell imaging of HUVEC cells costained with calcein-AM (live cells, green) and PI (dead cells, red) in different ICG solution concentrations. Scale bar: 50 μm.

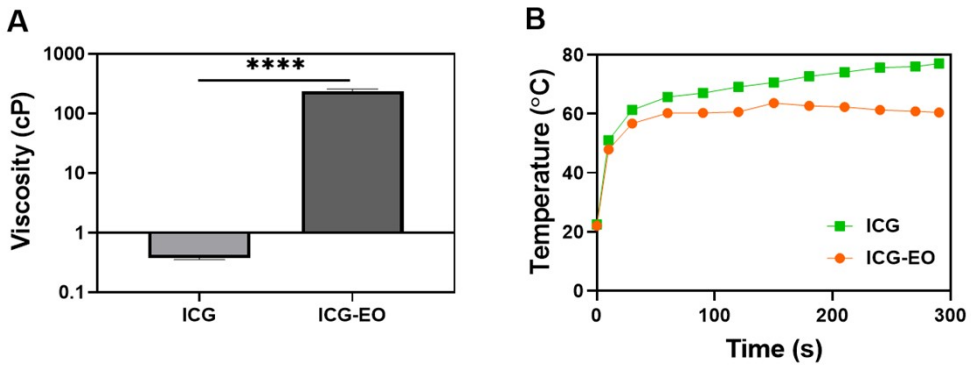

Figure S5. Comparison of viscosity and photothermal heating temperature of ICG solution and ICG-EO emulsion. (A) Viscosity of ICG-based photothermal agents at 37 °C. (B) Temperature of ICG-based photothermal agents containing 1290 μM ICG treated with 808 nm laser irradiation. Data are expressed as mean ± SD, n = 3. ****P < 0.0001.

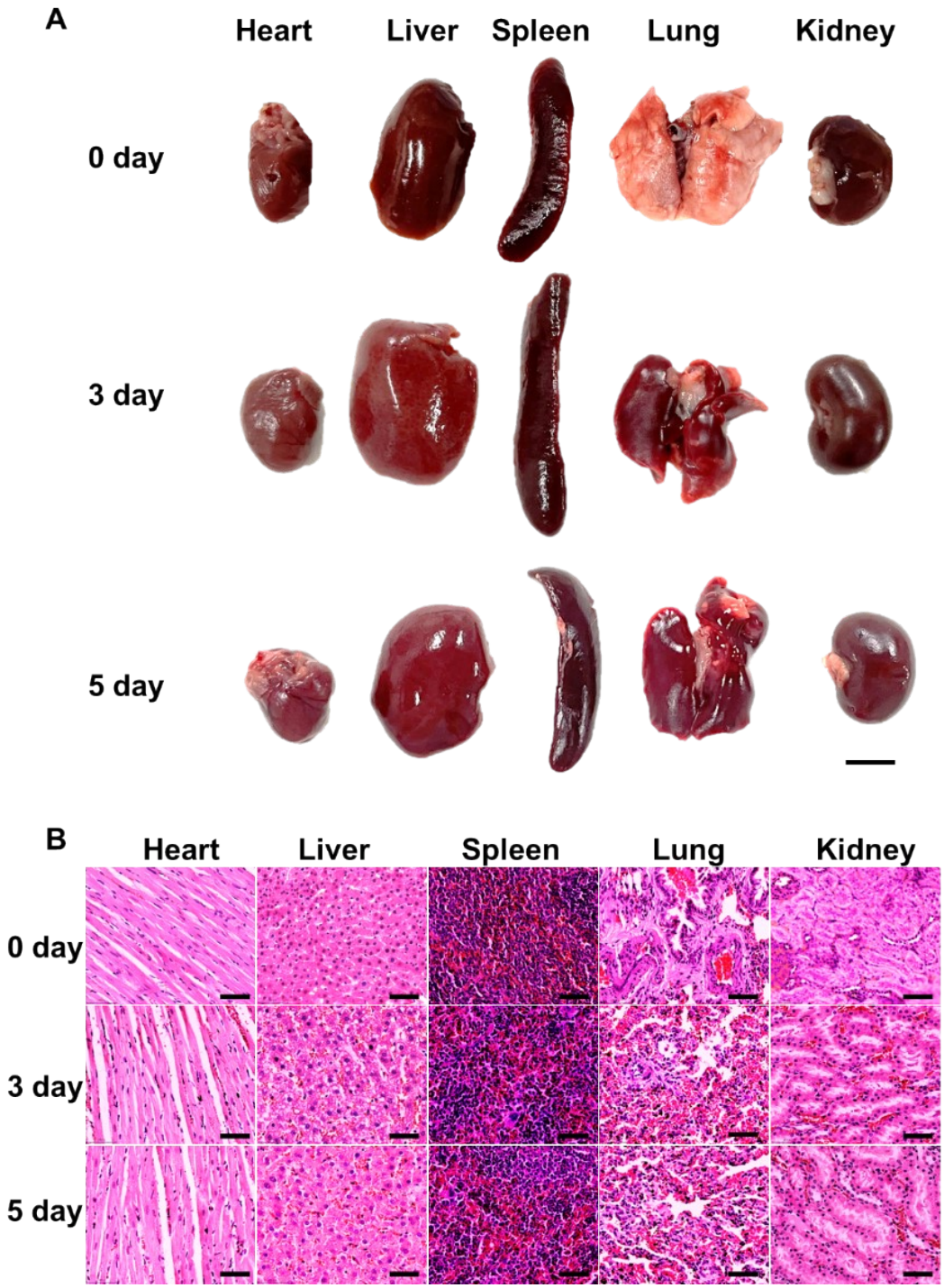

Figure S6. Histological analyses of major organs at 3 d and 5 d after Ti-PTT. (A) Macroscopic view, and (B) H&E staining. Scale bar: 1 cm (A) and 50 μm (B).

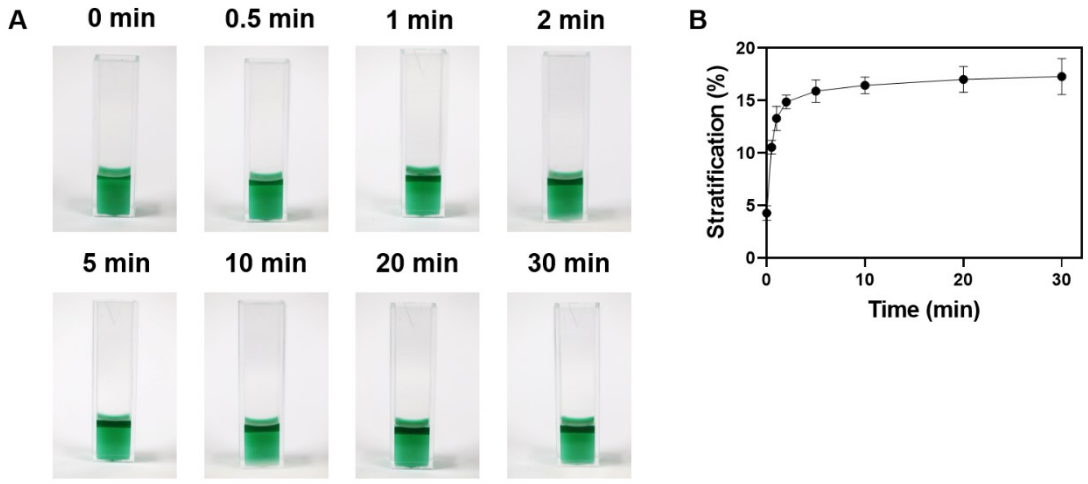

Figure S7. Stability test of ICG-EO emulsion. (A) Photographs of ICG-EO emulsion over time. (B) Stratification evaluation of the ICG-EO emulsion over time.

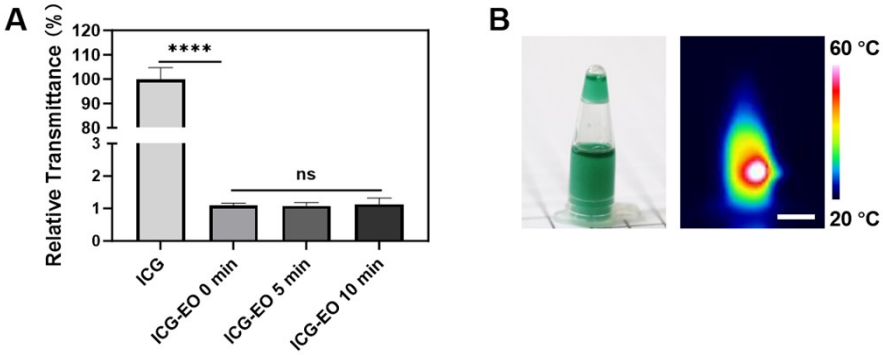

Figure S8. Transmittance and photothermal characterization of ICG-EO emulsion. (A) Relative transmittance at 800 nm normalized by ICG solution. (B) Photograph and Infrared imaging of ICG-EO emulsion treated with photothermal heating using 808 nm for 3 min. Data are expressed as mean ± SD, n = 3. ns ($p \geqslant 0.05$), and ****$P < 0.0001$. Scale bar: 5 mm (B).